NeuroImage: Clinical 23 (2019) 101910

Contents lists available at ScienceDirect

NeuroImage: Clinical

journal homepage: www.elsevier.com/locate/ynicl

Somatotopic organization of corticospinal/corticobulbar motor tracts in controls and patients with tumours: A combined fMRI–DTI study

Neven M. Hazzaa[a,b,*], Laura Mancini[a,c], John Thornton[a,c], Tarek A. Yousry[a,c]

[a] Lysholm Department of Neuro-radiology, National Hospital for Neurology and Neurosurgery, University College London Hospitals NHS Trust, WC1N 3BG, London, United Kingdom
[b] Menoufia University Hospital, Radiology Department Shebeen ElKoom, Menoufia, Egypt
[c] Academic Neuroradiological Unit, Institute of Neurology, University College of London, WC1N 3BG, London, United Kingdom

ARTICLE INFO

Keywords:
Functional MRI (fMRI)
Diffusion tensor imaging (DTI)
Corticospinal tract (CST)
Corticobulbar tract (CBT)
Brain tumours

ABSTRACT

Objectives: To investigate the relative somatotopic organization of the motor corticospinal/corticobulbar foot, hand, lip and tongue fascicles by combining fMRI with DTI and to examine the influence of subjacent intrinsic tumours on these fascicles.

Methods: The study was approved by the local ethics committee. Seven male and three female volunteers (median age: 35 years) and one female and eight male patients with brain tumours (median age: 37 years) were scanned on a 1.5-T MRI scanner. fMRI data, analysed using SPM5, identified the motor task-driven fMRI grey matter activations of the hand, foot, lips and tongue as seed regions for probabilistic tractography. The relationship between the components of the CST was assessed and the distances between them were measured. A statistical comparison was performed comparing these distances in the group of healthy hemispheres with those of the group of non-affected hemispheres and healthy hemispheres.

Results: Hand fascicles were identified in all subjects (38/38, 100%), followed by foot (32/38, 84%), lip (31/38, 81%) and tongue fascicles (28/38, 74%). At superior levels, the hand fascicles were anterolateral to the foot fascicles in 77–93% of healthy hemispheres (HH), in 50–71% of non-affected patients' hemispheres (pH) and in 67–89% of affected PH. At inferior levels, the hand fascicles were either anteromedial in 46–45% of HH or anterior in 75% of non-affected PH and in 67–83% of affected PH. Tongue and lip fascicles overlapped in 25–45% of HH, in 10–20% of non-affected PH and in 15–25% of affected PH. No significant difference was found between the group of affected hemispheres and that of healthy and non-affected hemispheres.

Conclusion: The somatotopy of the hand fascicles in relation to the foot fascicles was anterolateral in patients and volunteers at superior levels but anteromedial in volunteers and mostly anterior in patients at inferior levels. The lip and tongue fascicles generally overlapped. Intracranial tumours displaced the motor fascicles without affecting their relative somatotopy.

1. Introduction

Approximately 60% of corticospinal/corticobulbar tract (CST/CBT) fascicles originate in the primary motor cortex (M1) (Brodmann area 4) (Vulliemoz et al., 2005). The remaining fascicles originate from the non-primary motor cortex (Brodmann area 6) and from the parietal lobe (Dum and Strick, 1991; Ino et al., 2007; Lemon and Griffiths, 2005; Schulz et al., 2012). Although the somatotopy of major motor areas in the precentral gyrus (M1-motor homunculus) is well known (Penfield and Boldrey, 1937; Schieber, 2001), the somatotopy of the CST and CBT is less clear (Holodny et al., 2001; Park et al., 2008). Several diffusion tensor imaging (DTI)-based studies have observed differences in somatotopic organization. For instance, in the long axis of the corona radiata (CR) and the posterior limb of the internal capsule (PLIC), hand fascicles were either anterolateral to foot fascicles at the CR (Lee et al., 2014; Seo et al., 2012) and PLIC (Park et al., 2008) or anteromedial at

Abbreviations: CST/CBT, Corticospinal/Corticobulbar Tract; HH, Healthy Hemispheres; PH, Patients' Hemispheres; CR, Corona Radiata; CM, Cella Media; PLICs, Posterior Limb of the Internal Capsule-Superior; PLICi, Posterior Limb of the Internal Capsule-Inferior; AC, Anterior Commissure; CP, Cerebral Peduncle; ROIs, Seed Regions of Interest

* Corresponding author at: 61 Leyland Court, Angel Way, Romford RM1 1AF, United Kingdom.
E-mail addresses: neven.hazzaa@nhs.net (N.M. Hazzaa), lmancini@nhs.net (L. Mancini), john.thornton@ucl.ac.uk (J. Thornton), t.yousry@ucl.ac.uk (T.A. Yousry).

https://doi.org/10.1016/j.nicl.2019.101910
Received 29 August 2018; Received in revised form 16 May 2019; Accepted 24 June 2019
Available online 26 June 2019

the PLIC (Lee et al., 2012). Other studies found the hand fascicles to be anterolateral to the foot fascicles and partially overlapping relationships have been observed at lower levels (Holodny et al., 2005; Ino et al., 2007; Smits et al., 2007).

Previous studies used a conventional single-tensor DTI model (Holodny et al., 2005; Park et al., 2008; Smits et al., 2007), which cannot resolve the problem of crossing fibres (Akter et al., 2011). This problem has been addressed using probabilistic tractography (Lee et al., 2012, 2014; Seo et al., 2012). The necessary seed regions of interest (ROIs) required for the tracts dissection were identified manually either on the basis of anatomical landmarks (Hong et al., 2010; Kwon et al., 2011; Park et al., 2008; Seo et al., 2012) or through the application of functional magnetic resonance imaging (fMRI)-based methods. Using the latter, ROIs were placed in the white matter adjacent to the maximal fMRI activity (Smits et al., 2007), with some groups adding manually selected ROIs along the course of the CST (Holodny et al., 2005; Ino et al., 2007; Kim et al., 2008). In our study, we used a probabilistic DTI 2-tensor model, and selected grey matter ROIs in areas of maximal fMRI activation. Furthermore, we assessed both corticospinal and corticobulbar fascicles which we analysed at six sequential anatomical levels.

The aims of this study were to assess qualitatively and quantitatively the somatotopy of the motor fascicles of the hands, feet, lips and tongue at six sequential levels along the CST/CBT paths and to assess the effect of tumours on the relative somatotopy of these fascicles. We assessed the results of 1.5 T scans because these scanners are more ubiquitous and more common in operative suites.

2. Materials and methods

2.1. Subjects

The local ethics committee approved this retrospective study. All subjects provided written informed consent in accordance with the Declaration of Helsinki.

The study included a random selection of 10 healthy volunteers (7 males and 3 females, age range 26–41 years; median age 35 years) and 9 patients with intrinsic brain tumours (8 males and 1 female, age range 18–61 years; median age 37 years). Data were acquired from 2007 to 2009 and were retrospectively analysed.

Inclusion criteria were brain tumour patients in proximity to the CST/CBT.

2.2. MRI acquisition

All subjects were imaged on a 1.5-T Signa-Excite scanner (GE Healthcare, Milwaukee WI, USA) with the following sequences: coronal 3D-T1-weighted (T1w) fast spoiled gradient-echo (FSPGR) sequence (TI = 450 ms, $1.2 \times 1.2 \times 1.2$ mm^3); 3 DTI datasets, each with 25 diffusion directions (b = 1000 s/mm^2) and a single-shot spin-echo echo-planar-imaging (EPI) sequence (TE/TR = 91.5/10,000 ms, 33 contiguous axial slices parallel to the AC-PC line, 2x2x3 mm^3); 6 fMRI datasets with the following gradient-echo EPI sequence parameters: TE/TR = 50/4000 ms, 39-axial slices parallel to the anterior-posterior commissure-line, 3×3 mm^2 in-plane resolution, slice thickness = 2 mm, gap between slices = 1 mm.

2.3. fMRI paradigm

All subjects were trained to perform the various paradigms before the scanning session. The “block” design included 8 repetitions of alternating 20-s periods of self-paced movement tasks and rest; hands: finger-thumb opposition; feet: toe flexion/extension; lips: “pucker-up” with closed mouth to avoid major jaw movement-related artefacts; tongue: movement with the mouth closed to reduce jaw movement-related artefacts.

An Eloquence system (Invivo Corporation, Orlando, FL, USA) was used to present the paradigm.

2.4. Data processing and statistical analysis

2.4.1. fMRI analysis

fMRI data were analysed with SPM5 (www.fil.ion.ucl.ac.uk/spm/) as follows: 1-realignment with mean EPI calculation; 2-co-registration to the T1 image; 3-smoothing with a $6 \times 6 \times 6$ mm^3 full width at half maximum (FWHM) Gaussian kernel; and 4-estimation of the general linear model (GLM). The results were corrected for multiple comparisons with family-wise error (FWE) corrections thresholded at a *p*-value of 0.05. In 20% of the tasks (30/150), activation did not reach significance above this threshold; therefore, in these cases, uncorrected thresholds with non-task-specific *p*-values of 0.0005 (in 23/150 tasks “15.3%”) or uncorrected p-values of 0.001 (in 7/150 tasks “4.7%”) were used.

2.5. DTI analysis

2.5.1. ROI selection

The ROI selection was performed as follows: 1-T1w was segmented to obtain grey matter, white matter and cerebrospinal fluid maps. 2-The grey matter map was used as a mask to select the voxels with fMRI activations within the precentral gyrus's grey matter. 3-These voxels were co-registered with the mean EPI to the b = 0 diffusion data and were used as ROIs for tractography. The quality of the co-registration was visually assessed by overlaying the mean EPI in red onto the T1w and the mean EPI onto the b = 0 image, followed by thresholding EPI signals so that only the signal from the cerebrospinal fluid was visible. A maximum mismatch of 1 voxel from the cerebrospinal fluid in b = 0 and 2 voxels from the cerebrospinal fluid in T1w was defined as good coregistration. Two “termination” masks in each cerebral peduncle were selected for each subject. Finally, an “exclusion” mask was selected for each subject, including two sagittal regions in the midline of the brainstem and the corpus callosum. An example of the cortical ROIs is shown in Fig. 1.

2.5.2. Tractography

Fibre tracking was performed in two steps using FSL software (www.fmrib.ox.ac.uk/fsl/). First, the diffusion tensor was estimated at each voxel using a 2-tensor model. Second, 3D fibre tracking was performed using probabilistic tractography. Tract selection started from the ROI and terminated in the “termination” mask (beyond which no tracts continued). Streamlines that reached the “exclusion” masks were eliminated. The signal intensity (t-value) in the fMRI voxels represents the probability that the voxel is activated. As previously reported (Cherubini et al., 2007), the number of streamlines running from each voxel in the ROI was proportional to the t-value in each voxel and was normalised so that 5000 streamlines were always run from the voxel with the maximum t-value. The fibre-tracking analysis results were further normalised to the number of tracts that reached the termination mask, with the tract intensity in each voxel representing a “connectivity index”. Finally, the normalised tracts were warped to match the Montreal Neurological Institute (MNI) template (MNI152, 1-mm isotropic resolution) to enable between-subject comparisons.

2.5.3. Tract analysis

Six different axial slices were identified in MNI space: 1-level z = 32 mm (z-coordinate in MNI space) - corona radiata (CR); 2-level z = 23 mm-cella media (CM); 3-level z = 8 mm PLIC-superior (PLICs); 4-level z = −2 mm PLIC-inferior (PLICi); 5-level z = −7 mm anterior commissure (AC); and 6-level z = −12 mm cerebral peduncles (CP). At each level, we defined two perpendicular axes, in the anterior-posterior direction and in the medial-lateral direction with respect to the local anatomy rather than to the patient's head. These axes were defined at

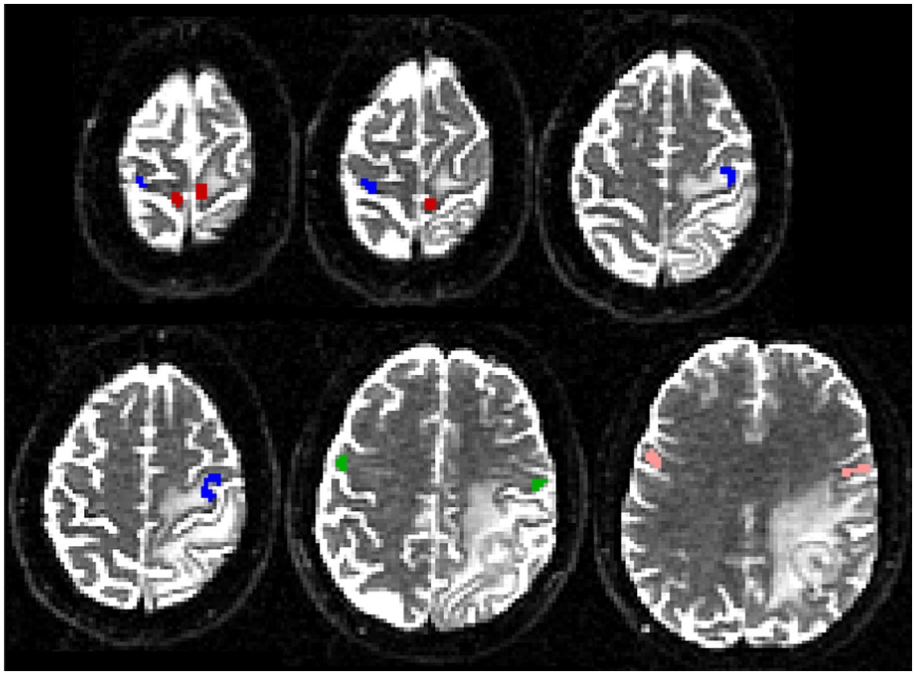

Fig. 1. Example of fMRI-based ROIs used as seed regions for tractography. Red = foot ROIs, blue = hand ROIs, green = lip ROIs, pink = tongue ROIs.

the various MNI z-levels and will be used to describe the observed fascicle arrangements (Fig. 2).

Locations of the centre of gravity (CoG) of the various CST components were calculated at the six anatomical levels mentioned above. Euclidean distances between the CoG of the various fascicles (foot-hand, foot-lip, foot-tongue, hand-lip, hand-tongue, lip-tongue) were also calculated. *t*-tests were performed to assess the differences in Euclidean distances in the affected hemispheres versus the combination of healthy and non-affected hemispheres. After a Bonferroni correction was applied to take into account the multiple statistical comparison, *p*-values below 0.008 were considered statistically significant.

The threshold for each fascicle was modified so that only the voxels with the highest connectivity index were visible. The different fascicles were considered overlapping if the voxels with the highest connectivity index had identical spatial coordinates, and they were considered separated if the voxels did not have the same spatial coordinates.

3. Results

The image distortion caused by susceptibility differences at the interface between the brain tissue and air-containing areas was limited and distant from the central brain area; therefore, this distortion did not affect the fMRI activation or the identification and display of the CST and CBT.

Tumours were identified above the level of the corona radiata (1 patient between z = 65 mm and z = 80 mm, 1 patient between z = 45 mm and z = 75 mm); at the level of the corona radiata (3 patients); at the levels of both the corona radiata and the cella media (3 patients); at the levels of CR, CM, PLICs and PLICi (1 patient).

3.1. fMRI

The expected fMRI activation pattern was observed in all subjects in the contralateral precentral and postcentral gyri and in the ipsilateral cerebellum.

In 120/150 tasks (80%), the activation persisted after correcting for multiple comparisons with FWE thresholding at a *p*-value of 0.05. In the remaining tasks (30/150; 20%), the activation persisted with the more sensitive uncorrected threshold p-value of 0.0005 in 23/150 tasks (15.3%), and in 7/150 tasks (4.7%), activation in the motor areas was only detectable with uncorrected *p*-values of 0.001.

3.2. Tractography

Overall, the hand related M1 CST fascicles were always identified (38/38, 100%), followed by the foot (32/38, 84%), lip (31/38, 81%) and tongue fascicles (28/38, 74%) (Table 1).

At least 2 separate motor fascicles were identified in all 38 hemispheres (100%). All four M1 CST components were identified in 17/38 (44.7%) hemispheres (Table 2).

3.3. Anatomic relationship of the CST fascicles

3.3.1. Foot and hand fascicles

3.3.1.1. Healthy controls. When considering only the foot (F) and hand (H) CST fascicles in healthy controls, the somatotopic arrangement was similar in both hemispheres, as summarised in Table 3.

The number of hemispheres in which the identified fascicles were separate ranged from 11/20 hemispheres at the level of the CP (z-level, −12 mm) to 14/20 hemispheres at the levels of CR, CM and PLICs (z-levels 32, 23 and 8 mm). The somatotopic arrangement was predominantly anterolateral at the most superior levels, ranging from 10/13 separate fascicles (77%) at the PLICi level to 13/14 separate fascicles (93%) at the CR level. When considering the anteromedial arrangement at the most inferior levels, 6/13 separate fascicles (46%) were identified at the AC level, and 5/11 separate fascicles (45%) were identified at the CP level (examples in Figs. 3 and 4).

3.3.1.2. Patients. In patients' non-affected hemispheres (Table 3), the foot and hand fascicles were (9/9; 100%) reconstructed at all levels. The number of hemispheres in which the identified fascicles were separate ranged from 7/9 hemispheres at the level of the PLICi (z-level, −2 mm) to 9/9 hemispheres at the CR and CM levels (z-levels 32 and 23, respectively). The somatotopic arrangement was mostly anterolateral at the most superior levels, ranging from 4/8 separate fascicles (50%) at the PLICs level to 7/9 separate fascicles (78%) at the CR and CM levels. The arrangement was mostly anterior at the most inferior levels, ranging from 5/7 separate fascicles (71%) at the PLICi

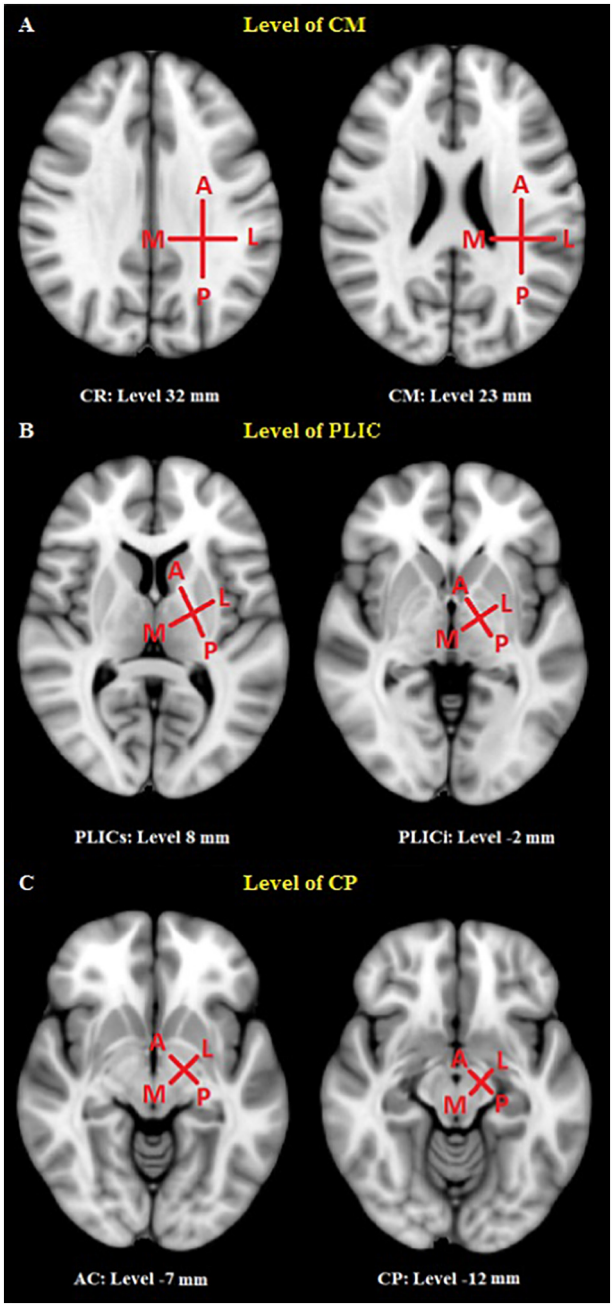

Fig. 2. Axial slices of the MNI template (MNI152, 1-mm isotropic resolution) at the levels of (a) the CM (CR and CM), (b) PLICs and PLICi and (c) CP (AC and CP), where the somatotopic arrangements of the CST/CBT fascicles were assessed. The lines labelled with AP and ML define the anterior-posterior and medial-lateral orientations, respectively, at the various levels used in the results to describe the fascicle arrangements. CR = corona radiata, CM = cella media, PLICs = posterior limb of the internal capsule-superior, PLICi = posterior limb of the internal capsule-inferior (PLICi), AC = anterior commissure, and CP = cerebral peduncles.

level to 6/8 separate fascicles (75%) at the AC and CP levels (examples in Fig. 5).

In patients' affected hemispheres (Table 3), the foot and hand fascicles were (9/9; 100%) reconstructed at all levels. The number of hemispheres in which the identified fascicles were separate ranged from 6/9 hemispheres (67%) at the most inferior levels (PLICs to CP, z-level 8 mm to −12 mm) to 9/9 hemispheres (100%) at the CR and CM levels (z-levels 32 and 23, respectively). The somatotopic arrangement was mostly anterolateral at the superior PLICs and PLICi levels (4/6

Table 1
Numbers of hemispheres and percentages of different fascicles that were identified in patients and controls.

Task	Patients – Affected Hemispheres		Patients – Non-Affected Hemispheres		Volunteers	
Number of hemispheres	Number/9	%	Number/9	%	Number/20	%
Hands	9	100	9	100	20	100
Feet	9	100	9	100	14	70
Lips	8	89	8	89	15	75
Tongue	6	67	7	78	15	75

Table 2
Percentages and numbers of hemispheres in which all or at least two motor tracts were identified in patients and controls.

	All 4 fascicles		At least 2 fascicles	
	Number	%	Number	%
Patients – affected hemispheres	6/9	67	9/9	100
Patients – non-affected hemispheres	5/9	56	9/9	100
Volunteers	6/20	30	20/20	100

separate fascicles; 67%) and at the CR (8/9 separate fascicles; 89%) and CM levels (7/9 separate fascicles; 78%). The arrangement was anterior at the inferior AC level (4/6 separate fascicles; 67%) and the CP level (5/6 separate fascicles; 83). In only one case, and only at the CM level, the hand was posterolateral to the foot fascicle.

The mean (standard deviation) Euclidean distances between the foot and hand fascicles ranged from 10.5 mm (CR) to 4 mm (CP) in the affected hemispheres and 9.4 mm (CR) to 4.2 mm (CP) in the group of healthy and non-affected hemispheres (Table 4). No statistically significant difference was found between the 2 groups.

3.3.2. Lip and tongue fascicles

3.3.2.1. Healthy controls. When considering only the lip (L) and tongue (T) CBT fascicles in healthy controls, the number of hemispheres in which the identified fascicles were separate ranged from 1/20 hemispheres (5%) at the CR level (z-level 32 mm) to 6/20 hemispheres (30%) at the CM level (z-level 23 mm) (Table 5). The number of hemispheres in which the L and T CBT fascicles overlapped ranged from 5/20 hemispheres (25%) at the CR level to 9/20 hemispheres (45%) at the CP level.

The somatotopic arrangement was predominantly overlapping and presented various arrangements when the fascicles were separated (Table 5).

3.3.2.2. Patients. In patients' non-affected hemispheres, the number of hemispheres in which the identified L and T CBT fascicles were separate ranged from 1/20 hemispheres (5%) at the CM level (z-level 23 mm) to 3/20 hemispheres (15%) at the PLICi and AC levels (z-levels −2 and − 7 mm, respectively). The number of hemispheres in which the L and T CBT fascicles overlapped ranged from 2/20 hemispheres (10%) at the PLICi and AC levels to 4/20 hemispheres (20%) at the CM and PLICs levels.

The somatotopic arrangement was mostly overlapping and presented various arrangements when the fascicles were separated (examples in Fig. 5).

In patients' affected hemispheres, the number of hemispheres in which the identified L and T CBT fascicles were separate ranged from 0 at the CR, CM and AC levels to 1/20 hemispheres (5%) at the other levels. The number of hemispheres in which the L and T CBT fascicles overlapped ranged from 3/20 hemispheres (15%) at the CR level to 5/20 hemispheres (25%) at the AC level.

Table 3
Summary of the numbers of hemispheres in which the foot and hand fascicles were identified, with their relative arrangements. Different colours are associated with the numbers specified in the table, ranging from a minimum of 0 (green) to a maximum of 13 (red). The various rows represent the six anatomical levels defined in Fig. 2. CR = corona radiata, CM = cella media, PLICs = posterior limb of the internal capsule-superior, PLICi = posterior limb of the internal capsule-inferior (PLICi), AC = anterior commissure, and CP = cerebral peduncles.

	Healthy Hemispheres					Non-Affected Patients' Hemispheres						Affected Patients' Hemispheres				
Level	Anteromedial	Anterior	Anterolateral	Overlap	Hand only	Medial	Anteromedial	Anterior	Anterolateral	Lateral	Overlapped	Anterior	Anterolateral	Lateral	Overlapped	No fibres
CR	0	1	13	0	6	0	1	0	7	1	0	0	8	1	0	0
CM	0	1	13	0	6	1	0	1	7	0	0	0	8	1	0	0
PLICs	0	2	12	0	6	1	0	3	4	0	1	2	4	0	3	0
PLICi	1	2	10	0	7	0	0	5	2	0	2	2	4	0	3	0
AC	6	3	4	0	7	0	0	6	1	1	1	4	2	0	3	0
CP	5	4	2	2	7	0	0	6	1	1	1	5	1	0	2	1

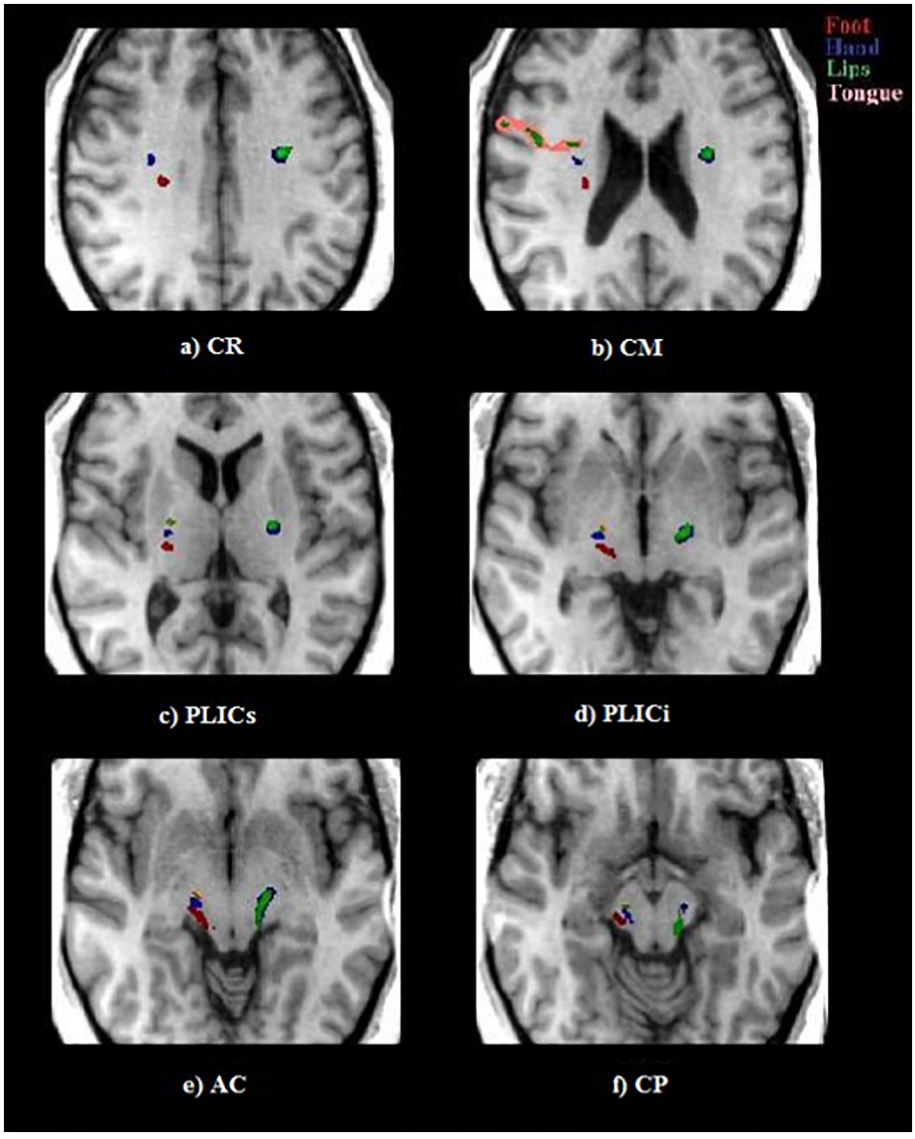

Fig. 3. Tractography maps of a healthy control overlaid in colour onto the axial MNI T1w template at the levels of the CR, CM, PLICs, PLICi, AC and PC. The colours encode the following different fascicles: red = foot, blue = hand, green = lips and pink = tongue. At the level of the CR (a), the foot fascicle is located in the posterior region of the right hemisphere, with the hand and lip fascicles located anterolateral to it. In the left hemisphere, only the hand and lip fascicles were reconstructed and overlap. At the CM level, the hand fascicles are located anterolateral to the foot fascicles in the right hemisphere. The tongue fascicles are located anterolateral to the foot, hand and lip fascicles. The hand and lip fascicles overlap in the left hemisphere. The somatotopic organization of these fascicles continues to be preserved with the same arrangement along the longitudinal axis of the PLIC at the levels of the PLICs (c) and PLICi (d). At the level of the AC (e), the foot fascicles are located in the posterior region, followed anteriorly by the hand, lip and tongue fascicles in the right hemisphere, whereas the lip and hand fascicles overlap in the left hemisphere.

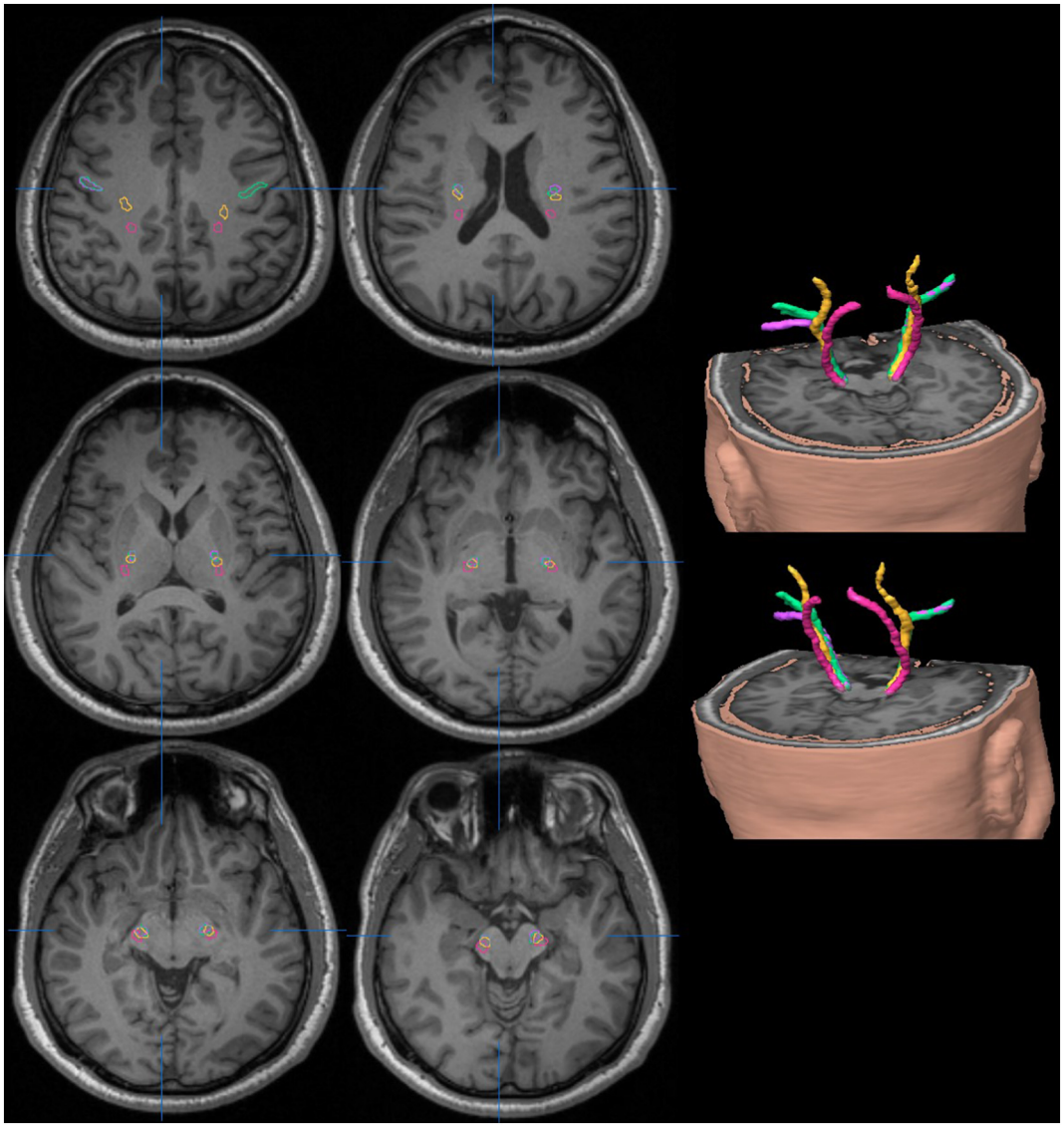

Fig. 4. Ttractography maps of a healthy control overlaid in colour onto the axial MNI T1W template at the levels of the CR (top row, left), CM (top row, right), PLICs (middle row, left), PLICi (middle row, right), AC (bottom row, left) and PC (bottom row, right). The colours encode the following different fascicles: pink = foot, yellow = hand, green = lips and purple = tongue. At the level of the CR (top row, left), the foot fascicle is located in the posterior region of the two hemispheres, with the hand and lip fascicles located anterolaterally. In the right hemisphere, the lip and tongue fascicles overlap, while in the left hemisphere, the tongue fascicles are at a more inferior level. At the CM level (top row, right), the hand fascicles are anterolateral to the foot fascicles in both hemispheres. The lip fascicles are located anterior to the hand fascicles. The tongue fascicle overlaps with the lip fascicle on the right hemisphere and is anterior to the lip fascicle (with some degree of overlap) on the left hemisphere. The somatotopic organization of these fascicles continues to be preserved with the same arrangement along the longitudinal axis of the PLIC at the levels of the PLICs (middle row, left) and PLICi (middle row, right), with some degree of overlap between the fascicles. At the level of the AC (bottom left), the foot fascicles are located posteriorly, followed anteriorly by the hand; lip and tongue fascicles overlap in the right hemisphere, and to a lesser degree in the left hemisphere. The 3D reconstructions represent the same tracts.

The somatotopic arrangement was predominantly overlapping and presented various arrangements when the fascicles were separated (examples in Fig. 5).

The mean (standard deviation) Euclidean distances between the lip and tongue fascicles ranged from 3.5 mm (CR) to 1.1 mm (CP) in the affected hemispheres and 4.7 mm (CR) to 1.8 mm (CP) in the group of healthy and non-affected hemispheres (Table 6). No statistically significant difference was found between the 2 groups.

Euclidean distances were also calculated for the combination of the various fascicles (Table 7). No statistically significant differences were found between the group of affected hemispheres and that of healthy and non-affected hemispheres.

4. Discussion

In this study, we used fMRI and probabilistic DTI to define the somatotopic organization of the foot, hand, lip and tongue fascicles of the CST/CBT. Our reference line was the long axis of six sequential slices of the MNI template. We found the hand to be anterolateral to foot fascicles at the superior levels in 77–93% of healthy hemispheres (HH), in 50–71% of non-affected patients' hemispheres (PH) and in 67–89% of affected PH. At the inferior levels, the hand fascicles were anteromedial to foot fascicles in 45–46% of HH or anterior to them in 75% of non-affected PH and in 67–83% of affected PH. The tongue and lip fascicles overlapped in 25–45% of HH, in 10–20% of non-affected PH and in 15–25% of affected PH. In almost all cases, the tumour displaced the CST/CBT without altering their somatotopy.

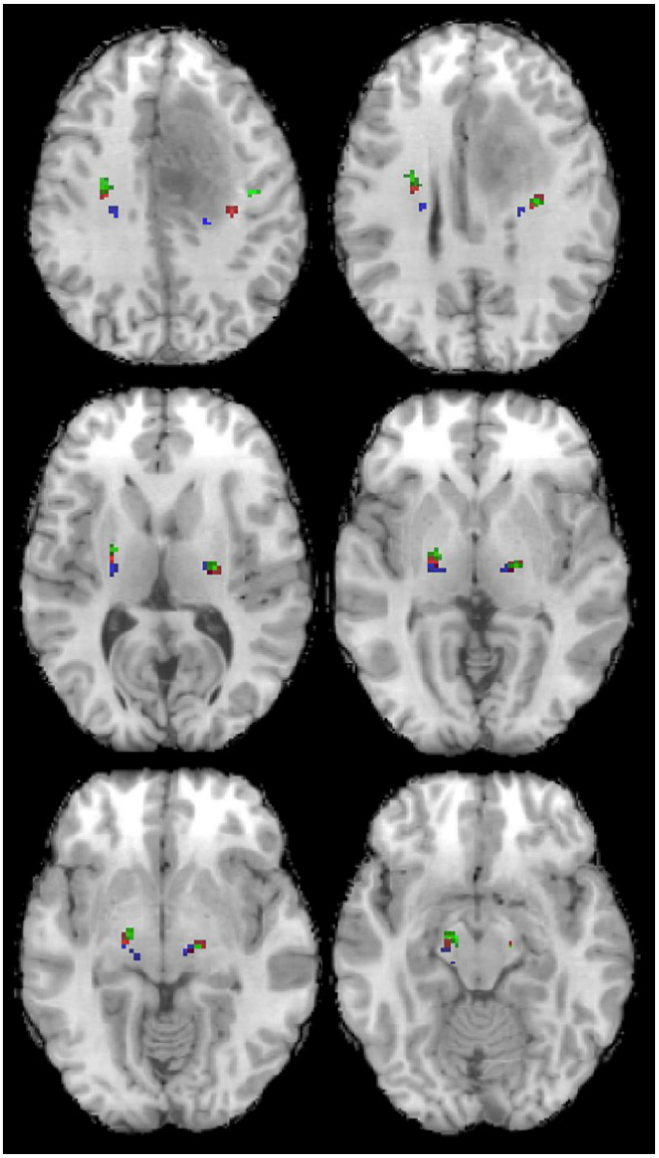

Fig. 5. A patient with the left superior frontal glioma located within the vicinity of the left CST/CBT. The figure shows T1w axial slices with overlaid fibre tractography maps depicted in colour. The images were normalised to the MNI template. The selected slices are presented at the levels of the CR (top left), CM (top right), PLICs (middle left), PLICi (middle right), AC (bottom left) and CP (bottom right). At the level of the CR (top left), the hand fascicles (red) are located anterolateral to the foot fascicles (blue) in both affected and non-affected hemispheres. However, in the affected hemisphere, these fascicles are displaced posteriorly and laterally. At the level of CM (top left), the CST/CBT fascicular components are somatotopically arranged with the foot fascicles in a posterior position, followed anterolaterally by the hand fascicles and the lip fascicles (tongue fascicles were not identified in this case). In the affected hemisphere, the different CST/CBT fascicular components are displaced by the tumours, yet their somatotopic organization is preserved. At the PLICs (middle left) and PLICi (middle right) levels, the fascicles are arranged from posterior to anterior in the non-affected hemisphere, with the foot fascicle located in the posterior region, followed by the hand and lip fascicles. In the affected hemisphere, the foot fascicles are medial, while hand and lip fascicles overlap and are lateral to the foot fascicles. At the level of the AC (bottom left), these fascicles are again somatotopically organised in the non-affected hemisphere, with the foot fascicles located in the most posterior aspect, followed anteriorly by the hand and lip fascicles. All three fascicles overlap in the affected hemisphere.

Table 4
Mean (standard deviation) of Euclidean distances between foot and hand fascicles of the corticospinal tract. CR = corona radiata, CM = cella media, PLICs = posterior limb of the internal capsule-superior, PLICi = posterior limb of the internal capsule-inferior (PLICi), AC = anterior commissure, and CP = cerebral peduncles.

	Affected hemispheres	Healthy and non-affected hemispheres	p-values
CR	10.5 (3.9)	9.4 (2.4)	0.51
CM	9.7 (4.1)	8.9 (3.1)	0.68
PLICs	5.1 (3.3)	5.0 (2.1)	0.98
PLICi	3.4 (2.3)	4.4 (1.8)	0.30
AC	3.7 (2.1)	4.5 (1.9)	0.43
CP	4.0 (3.1)	4.2 (1.9)	0.92

Our study benefited from the use of 2 tensor probabilistic fibre-tracking, the limited operator input in selecting ROIs, the identification of both CST and CBT, and the identification of the fibre arrangements at six sequential anatomical levels.

Although the somatotopic organization in the cortical homunculus is well established (Penfield and Boldrey, 1937; He et al., 1993; Schieber, 2001), it remains controversial within the CST/CBT (Holodny et al., 2005; Park et al., 2008). Two patterns of organization have been described at the PLIC level in studies combining fMRI and tractography. Using the orientation convention used in the present paper (Fig. 2), the hand was described to be either lateral (Holodny et al., 2005; Ino et al., 2007) or anterior to the foot fascicle (Ino et al., 2007; Lee et al., 2012; Park et al., 2008). A study using direct white matter electrical stimulation in the PLIC area reported a face-anterior, arm-intermediate and leg-posterior somatotopic organization (Duerden et al., 2011). Ffurther fMRI/tractography studies described the pattern at the centrum semiovale level (hand anterolateral to foot fascicles, Seo et al., 2012), and at the CP level (hand anterolateral to foot fascicles, Kwon et al., 2011).

To the best of our knowledge, lip and tongue fascicular organization has not been previously investigated together using fMRI-DTI; only the lip fascicle was reconstructed, and was located at the PLIC level anterior to the hand and foot fascicles (Smits et al., 2007). In in our study, the lip and tongue fascicles were visualised less frequently than the hand and foot fascicles, in part because they are simply not present at some of the superior levels. Another explanation relates to the limitations of probabilistic tractography, which does not always overcome the issue of crossing and kissing fibres (Jones, 2008) as happens when these fascicles cross the superior longitudinal fasciculus.

We successfully distinguished the somatotopic organization of the CST/CBT in healthy volunteers and patients. Along the long- axis of the superior levels (CM-PLIC), the hand fascicles were anterolateral to the foot fascicles in 77–93% of HH and anteromedial at the inferior levels (AC-CP) in 45–46% of HH. The tongue and lip fascicles overlapped at all levels in 25–45% of HH. These findings are consistent with the patterns described in previous studies in which the hand fascicles were anterolateral to the foot fascicles along the long axis at the CR (Lee et al., 2014; Seo et al., 2012) and PLIC levels (Park et al., 2008). Using a different approach, other studies have described the reference line along the PLIC' short axis, with the hand medial to foot fascicles (Park et al., 2008). The tongue and lip fascicles generally overlapped at all levels which is consistent with previous work showing that body part representations closer to each other are more likely to overlap (Duerden et al., 2011)

At the midbrain level, variable arrangements were observed with the hand anteromedial to foot fascicles in 46–45% of HH. Other studies found the hand fascicles medial to the foot fascicles (Hong et al., 2010; Kwon et al., 2011; Park et al., 2008). Some studies used operator-dependent methods by selecting ROIs based on either known anatomical landmarks (Akter et al., 2011; Holodny et al., 2005; Hong et al., 2010; Kwon et al., 2011; Park et al., 2008; Seo et al., 2012) or partially operator-dependent fMRI-driven methods (Hattingen et al., 2009;

Table 5
Summary of the number of hemispheres in which the lip and tongue fascicles were identified, with their relative arrangements. Different colours are associated with the numbers specified in the table, ranging from a minimum of 0 (green) to a maximum of 9 (red). The various rows represent the six anatomical levels defined in Fig. 2. CR = corona radiata, CM = cella media, PLICs = posterior limb of the internal capsule-superior, PLICi = posterior limb of the internal capsule-inferior (PLICi), AC = anterior commissure, and CP = cerebral peduncles.

	Healthy Hemispheres							Non-affected Patients' Hemispheres								Affected Patients' Hemispheres					
Level	Anteromedial	Anterior	Anterolateral	Overlap	Lip only	Tongue only	No fibres	Medial	Anterior	Anterolateral	Lateral	Overlapped	Lip only	Tongue only	No fibres	Anteromedial	Anterolateral	Overlapped	Lip only	Tongue only	No fibres
CR	1	0	0	5	6	2	6	1	0	0	1	3	2	1	1	0	0	3	3	0	3
CM	1	1	3	7	2	2	3	0	0	1	0	4	2	1	1	0	0	4	3	1	1
PLICs	1	2	2	6	3	2	4	0	1	1	0	4	2	1	0	0	1	4	3	0	1
PLICi	2	2	1	7	3	2	4	0	3	0	0	2	2	1	1	0	1	4	3	0	1
AC	2	1	2	7	3	2	4	0	2	1	0	2	2	1	1	0	0	5	3	0	1
CP	1	1	0	9	3	2	4	0	1	1	0	3	3	0	1	1	0	4	3	0	1

Table 6
Mean (standard deviation) of Euclidean distances between lip and tongue fascicles. CR = corona radiata, CM = cella media, PLICs = posterior limb of the internal capsule-superior, PLICi = posterior limb of the internal capsule-inferior (PLICi), AC = anterior commissure, and CP = cerebral peduncles.

	Affected hemispheres	Healthy and non-affected hemispheres	p-values
CR	3.5 (2.0)	4.7 (4.6)	0.50
CM	6.5 (7.9)	3.8 (4.9)	0.49
PLICs	1.0 (1.0)	2.4 (2.9)	0.12
PLICi	1.0 (1.0)	1.9 (2.1)	0.20
AC	1.5 (1.5)	1.8 (2.1)	0.69
CP	1.1 (1.4)	1.8 (2.4)	0.45

Holodny et al., 2001; Ino et al., 2007; Kim et al., 2008; Lee et al., 2012, 2014; Radmanesh et al., 2015; Schonberg et al., 2006; Smits et al., 2007). In these methods, ROIs were manually selected by choosing the white matter voxels either closest to the fMRI activation (Hattingen et al., 2009; Holodny et al., 2001; Radmanesh et al., 2015; Schonberg et al., 2006; Smits et al., 2007) or at different locations along the CST in combination with fMRI-driven ROIs (Holodny et al., 2001; Ino et al., 2007; Kim et al., 2008; Lee et al., 2012, 2014; Radmanesh et al., 2015; Schonberg et al., 2006; Smits et al., 2007). Care needs also to be taken when selecting ROIs on the basis of known anatomical landmarks as their identification can be limited by their inter-individual variability and potential distortion by adjacent brain tumours thereby limiting the precision of this approach (Hong et al., 2010; Ino et al., 2007; Kim et al., 2008; Park et al., 2008; Schonberg et al., 2006; Seo et al., 2012; Smits et al., 2007; Thomas et al., 2005). Furthermore, with the exception of the hand motor area 'hand-knob' the motor areas of the precentral gyrus lack clear anatomical landmarks (Yousry et al., 1995a, 1995b). An operator-independent ROI selection proposed by Cherubini et al. defined ROIs on the basis of the maximal fMRI activation (Cherubini et al., 2007). We adapted the method by restricting the ROI to the grey matter voxels of the precentral gyrus within the fMRI activation area.

Conventional DTI has limited applications due to the crossing fibre problem, which can be largely overcome by the probabilistic DTI from the FSL package (Abhinav et al., 2014; Akter et al., 2011; Lee et al., 2014; Smits et al., 2007; Thomas et al., 2005; Zhang et al., 2012).

In our study, we used a probabilistic DTI 2-tensor model, which largely addressed the crossing fibres problem that affected the previously used single-tensor model (Akter et al., 2011; Smits et al., 2007; Thomas et al., 2005). As a result, CBT components traversed by the longitudinal fasciculus were identified in most cases and in proximity to the tumours.

Several studies have examined the effects of tumours on nearby tracts (Holodny et al., 2001; Schonberg et al., 2006; Smits et al., 2007). In our study, we found that tumours displaced the entire adjacent tract without altering its somatotopy (Tables 3 and 4). The present results may therefore contribute to the pre-surgical assessment and inform clinical practice.

Despite the aforementioned improvements, our method localised the tongue and lip fascicles in 5–45% of subjects. In some cases, tractography stopped at the longitudinal fasciculus level or reproduced artefactual tracts. Improved tracking methods and data acquisition in stronger 3 T magnetic fields and with more diffusion directions (60 or

Table 7
Mean (standard deviation) [*p*-values] of Euclidean distances between fascicles: FL = foot-lips, FT = foot-tongue, HL = hand-lips, HT = hand-tongue. CR = corona radiata, CM = cella media, PLICs = posterior limb of the internal capsule-superior, PLICi = posterior limb of the internal capsule-inferior (PLICi), AC = anterior commissure, and CP = cerebral peduncles.

	Affected hemispheres				Healthy and non-affected hemispheres			
	FL	FT	HL	HT	FL	FT	HL	HT
CR	20.4 (9.4)	17.9 (7.5)	12.1 (7.9)	10.0 (8.2)	16.1 (7.6) [0.36]	18.8 (7.7) [0.81]	6.5 (5.8) [0.16]	10.6 (6.6) [0.88]
CM	12.8 (5.1)	16.6 (8.8)	5.1 (2.6)	9.3 (7.2)	12.5 (5.5) [0.92]	13.2 (5.0) [0.41]	4.9 (5.3) [0.92]	7.4 (5.8) [0.57]
PLICs	5.0 (2.6)	6.3 (4.3)	1.8 (1.6)	2.3 (1.1)	7.9 (3.2) [0.06]	7.0 (2.6) [0.76]	3.1 (2.7) [0.16]	3.6 (1.8) [0.06]
PLICi	3.3 (1.7)	4.0 (2.7)	1.7 (1.4)	1.9 (0.7)	5.0 (1.6) [0.07]	4.9 (1.6) [0.47]	2.5 (2.0) [0.26]	2.6 (1.2) [0.11]
AC	3.3 (1.9)	4.0 (2.2)	2.1 (1.7)	1.9 (0.7)	5.2 (1.9) [0.07]	5.5 (2.0) [0.18]	2.6 (2.0) [0.58]	2.6 (1.4) [0.15]
CP	3.4 (3.8)	4.4 (3.6)	1.5 (1.2)	1.5 (0.7)	5.4 (2.3) [0.31]	5.0 (1.4) [0.71]	2.5 (2.6) [0.20]	2.2 (1.6) [0.12]

more), larger diffusion gradients (b-values of 2500–3000 s/mm^2) and possibly several b-values could overcome this problem (Reisert et al., 2011).

Another promising approach is the use of arterial spin labelling-based fMRI (Brown et al., 2007) or transcranial magnetic stimulation (TMS). TMS locates the signal at a neuronal level, allowing a high-resolution physiological approach. The confounders of this technique include the scalp-to-cortex distance and that the TMS pulse may depend not only on activation at the site of the stimulus but also depend on direct responses from remote areas of the cortex (Siebner et al., 2009). The fMRI signal is related to the blood flow and blood oxygenation rather than directly to neuronal activation and as such is an indirect measurement of neuronal activity, leading to a potential spatial discrepancy. fMRI, however, has the advantage of a reduced operator dependency compared to TMS and of being widely available and used in the clinical environment; therefore, it is easy to integrate into the clinical routine pathway, especially for presurgical planning for intracerebral tumours.

The main limitation of our study results from the use of a 1.5 T scanner rather than a 3 T scanner. A higher field strength improves the signal-to-noise ratio and thereby the fMRI blood oxygen level-dependent (BOLD) signal. This signal is also less affected by the venous compartments, providing a more specific localization in the grey matter (Garcia-Eulate et al., 2011). Recent hardware and software improvements also allow the use of DTI sequences with a higher number of directions, larger b-values and multiple b-values in 5–10 min acquisitions, thereby improving the reliability of the results. However, our results also show that it is possible to discriminate the fascicles at the more ubiquitous field strength of 1.5 T.

5. Conclusions

The fMRI and DTI technique applied here enables reliable identification of the somatotopic organization of the principal motor pathways at the most commonly used field strength of 1.5 T. The predominant somatotopic organization within the CST was for the hand fascicle to be located anterolateral to the foot fascicle along the long axis of the CR and PLIC at the most superior levels and anteromedial to the foot fascicles at the most inferior levels (CP). The arrangement of the tongue and lip fascicles predominantly overlapped at all levels.

In the majority of cases assessed in this study, the mass effect of tumours led to the displacement of the fascicles, without affecting their relative organization.

Acknowledgements

This research study was supported by the National Institute for Health Research, University College of London Hospital, Biomedical Research Centre.

Funding

This study has received funding from the Egyptian government and a Citadel Capital scholarship sponsoring Dr. Neven M. Hazzaa in the UK.

Declaration of Competing Interest

None.

References

Abhinav, K., Yeh, F.C., Pathak, S., Suski, V., Lacomis, D., Friedlander, R.M., Fernandez-Miranda, J.C., 2014. Advanced diffusion MRI fiber tracking in neurosurgical and neurodegenerative disorders and neuroanatomical studies: a review. Biochim. Biophys. Acta 1842, 2286–2297. https://doi.org/10.1016/j.bbadis.2014.08.002.

Akter, M., Hirai, T., Sasao, A., Nishimura, S., Uetani, H., Iwashita, K., Yamashita, Y., 2011. Multi-tensor tractography of the motor pathway at 3T: a volunteer study. Magn. Reson. Med. Sci. 10, 59–63. https://doi.org/10.2463/mrms.10.59.

Brown, G.G., Perthen, J.E., Liu, T.T., Buxton, R.B., 2007. A primer on functional magnetic resonance imaging. Neuropsychol. Rev. 17, 107–125. https://doi.org/10.1007/s11065-007-9028-8.

Cherubini, A., Luccichenti, G., Peran, P., Hagberg, G.E., Barba, C., Formisano, R., Sabatini, U., 2007. Multimodal fMRI tractography in normal subjects and in clinically recovered traumatic brain injury patients. Neuroimage 34, 1331–1341. https://doi.org/10.1016/j.neuroimage.2006.11.024.

Duerden, E.G., Finnis, K.W., Peters, T.M., Sadikot, A.F., 2011. Three-dimensional somatotopic organization and probabilistic mapping of motor responses from the human internal capsule. J. Neurosurg. 114, 1706–1714. https://doi.org/10.3171/2011.1.jns10136.

Dum, R.P., Strick, P.L., 1991. The origin of corticospinal projections from the premotor areas in the frontal lobe. J. Neurosci. 11, 667–689. https://doi.org/10.1523/JNEUROSCI.11-03-00667.1991.

Garcia-Eulate, R., Garcia-Garcia, D., Dominguez, P.D., Noguera, J.J., De Luis, E., Rodriguez-Oroz, M.C., Zubieta, J.L., 2011. Functional bold MRI: advantages of the 3 T vs. the 1.5 T. Clin. Imaging 35, 236–241. https://doi.org/10.1016/j.clinimag.2010.07.003.

Hattingen, E., Rathert, J., Jurcoane, A., Weidauer, S., Szelenyi, A., Ogrezeanu, G., Seifert, V., Zanella, F.E., Gasser, T., 2009. A standardised evaluation of pre-surgical imaging of the corticospinal tract: where to place the seed ROI. Neurosurg. Rev. 32, 445–456. https://doi.org/10.1007/s10143-009-0197-1.

He, S.Q., Dum, R.P., Strick, P.L., 1993. Topographic organization of corticospinal projections from the frontal lobe: motor areas on the lateral surface of the hemisphere. J. Neurosci. 13, 952–980. https://doi.org/10.1523/JNEUROSCI.13-03-00952.1993.

Holodny, A.I., Ollenschleger, M.D., Liu, W.C., Schulder, M., Kalnin, A.J., 2001. Identification of the corticospinal tracts achieved using blood-oxygen-level-dependent and diffusion functional MR imaging in patients with brain tumors. AJNR Am. J. Neuroradiol. 22, 83–88.

Holodny, A.I., Watts, R., Korneinko, V.N., Pronin, I.N., Zhukovskiy, M.E., Gor, D.M., Ulug, A., 2005. Diffusion tensor tractography of the motor white matter tracts in man: current controversies and future directions. Ann. N. Y. Acad. Sci. 1064, 88–97. https://doi.org/10.1196/annals.1340.016.

Hong, J.H., Son, S.M., Jang, S.H., 2010. Somatotopic location of corticospinal tract at pons in human brain: a diffusion tensor tractography study. Neuroimage 51, 952–955. https://doi.org/10.1016/j.neuroimage.2010.02.063.

Ino, T., Nakai, R., Azuma, T., Yamamoto, T., Tsutsumi, S., Fukuyama, H., 2007. Somatotopy of corticospinal tract in the internal capsule shown by functional MRI and diffusion tensor images. Neuroreport 18, 665–668. https://doi.org/10.1097/WNR.0b013e3280d943e1.

Jones, D.K., 2008. Studying connections in the living human brain with diffusion MRI. Cortex 44, 936–952. https://doi.org/10.1016/j.cortex.2008.05.002.

Kim, Y.H., Kim, D.S., Hong, J.H., Park, C.H., Hua, N., Bickart, K.C., Byun, W.M., Jang, S.H., 2008. Corticospinal tract location in internal capsule of human brain: diffusion tensor tractography and functional MRI study. Neuroreport 19, 817–820. https://doi.org/10.1097/WNR.0b013e328300a086.

Kwon, H.G., Hong, J.H., Jang, S.H., 2011. Anatomic location and somatotopic arrangement of the corticospinal tract at the cerebral peduncle in the human brain. Am. J. Neuroradiol. 32, 2116–2119. https://doi.org/10.3174/ajnr.A2660.

Lee, D.H., Kwon, Y.H., Hwang, Y.T., Kim, J.H., Park, J.W., 2012. Somatotopic location of corticospinal tracts in the internal capsule with MR tractography. Eur. Neurol. 67, 69–73. https://doi.org/10.1159/000334097.

Lee, D.H., Hong, C., Han, B.S., 2014. Diffusion-tensor magnetic resonance imaging for hand and foot fibers location at the corona radiata: comparison with two lesion studies. Front. Hum. Neurosci. 8, 752. https://doi.org/10.3389/fnhum.2014.00752.

Lemon, R.N., Griffiths, J., 2005. Comparing the function of the corticospinal system in different species: organizational differences for motor specialization? Muscle Nerve 32, 261–279. https://doi.org/10.1002/mus.20333.

Park, J.K., Kim, B.S., Choi, G., Kim, S.H., Choi, J.C., Khang, H., 2008. Evaluation of the somatotopic organization of corticospinal tracts in the internal capsule and cerebral peduncle: results of diffusion-tensor MR tractography. Korean J. Radiol. 9, 191–195. https://doi.org/10.3348/kjr.2008.9.3.191.

Penfield, W., Boldrey, E., 1937. Somatic motor and sensory representation in the cerebral cortex of man as studied by electrical stimulation. Brain 60, 389–443. https://doi.org/10.1093/brain/60.4.389.

Radmanesh, A., Zamani, A.A., Whalen, S., Tie, Y., Suarez, R.O., Golby, A.J., 2015. Comparison of seeding methods for visualization of the corticospinal tracts using single tensor tractography. Clin. Neurol. Neurosurg. 129, 44–49. https://doi.org/10.1016/j.clineuro.2014.11.021.

Reisert, M., Mader, I., Anastasopoulos, C., Weigel, M., Schnell, S., Kiselev, V., 2011. Global fiber reconstruction becomes practical. Neuroimage 54, 955–962. https://doi.org/10.1016/j.neuroimage.2010.09.016.

Schieber, M.H., 2001. Constraints on somatotopic organization in the primary motor cortex. J. Neurophysiol. 86, 2125–2143. https://doi.org/10.1152/jn.2001.86.5.2125.

Schonberg, T., Pianka, P., Hendler, T., Pasternak, O., Assaf, Y., 2006. Characterization of displaced white matter by brain tumors using combined DTI and fMRI. Neuroimage 30, 1100–1111. https://doi.org/10.1016/j.neuroimage.2005.11.015.

Schulz, R., Park, C.H., Boudrias, M.H., Gerloff, C., Hummel, F.C., Ward, N.S., 2012. Assessing the integrity of corticospinal pathways from primary and secondary cortical motor areas after stroke. Stroke 43, 2248–2251. https://doi.org/10.1161/strokeaha.112.662619.

Seo, J.P., Chang, P.H., Jang, S.H., 2012. Anatomical location of the corticospinal tract

according to somatotopies in the centrum semiovale. Neurosci. Lett. 523, 111–114. https://doi.org/10.1016/j.neulet.2012.06.053.
Siebner, H.R., Hartwigsen, G., Kassuba, T., Rothwell, J.C., 2009. How does transcranial magnetic stimulation modify neuronal activity in the brain? Implications for studies of cognition. Cortex 45, 1035–1042. https://doi.org/10.1016/j.cortex.2009.02.007.
Smits, M., Vernooij, M.W., Wielopolski, P.A., Vincent, A.J., Houston, G.C., Van der Lugt, A., 2007. Incorporating functional MR imaging into diffusion tensor tractography in the preoperative assessment of the corticospinal tract in patients with brain tumors. AJNR Am. J. Neuroradiol. 28, 1354–1361. https://doi.org/10.3174/ajnr.A0538.
Thomas, B., Eyssen, M., Peeters, R., Molenaers, G., Van Hecke, P., De Cock, P., Sunaert, S., 2005. Quantitative diffusion tensor imaging in cerebral palsy due to periventricular white matter injury. Brain 128, 2562–2577. https://doi.org/10.1093/brain/awh600.
Vulliemoz, S., Raineteau, O., Jabaudon, D., 2005. Reaching beyond the midline: why are human brains cross wired? Lancet Neurol. 4, 87–99. https://doi.org/10.1016/s1474-4422(05)00990-7.
Yousry, T., Schmid, U.D., Schmidt, D., Heiss, D., Jassoy, A., Eisner, W., Reulen, H.J., Reiser, M., 1995a. The motor hand area. Noninvasive detection with functional MRI and surgical validation with cortical stimulation. Radiologe 35, 252–255.
Yousry, T.A., Schmid, U.D., Jassoy, A.G., Schmidt, D., Eisner, W.E., Reulen, H.J., Reiser, M.F., Lissner, J., 1995b. Topography of the cortical motor hand area: prospective study with functional MR imaging and direct motor mapping at surgery. Radiology 195, 23–29. https://doi.org/10.1148/radiology.195.1.7892475.
Zhang, H., Schneider, T., Wheeler-Kingshott, C.A., Alexander, D.C., 2012. NODDI: practical in vivo neurite orientation dispersion and density imaging of the human brain. Neuroimage 61, 1000–1016. https://doi.org/10.1016/j.neuroimage.2012.03.072.